Received: 12 April 2020 | Revised: 27 February 2021 | Accepted: 8 March 2021

DOI: 10.1096/fj.202000856R

RESEARCH ARTICLE

THE FASEB JOURNAL

Evolutionary and functional analyses demonstrate conserved ferroptosis protection by *Arabidopsis* GPXs in mammalian cells

Wangyang Song[1,2] | **Shan Xin**[3] | **Meng He**[1] | **Susanne Pfeiffer**[3] | **Aiping Cao**[2] | **Hongbin Li**[2] | **Joel A. Schick**[3] | **Xiang Jin**[1,2]

[1]Ministry of Education Key Laboratory for Ecology of Tropical Islands, Key Laboratory of Tropical Animal and Plant Ecology of Hainan Province, College of Life Sciences, Hainan Normal University, Haikou, China

[2]Key Laboratory of Xinjiang Phytomedicine Resource and Utilization of Ministry of Education, College of Life Sciences, Shihezi University, Shihezi, China

[3]Institute of Molecular Toxicology and Pharmacology, Genetics and Cellular Engineering Group, Helmholtz Zentrum Munich, Neuherberg, Germany

Correspondence
Joel A. Schick, Institute of Molecular Toxicology and Pharmacology, Genetics and Cellular Engineering Group, Helmholtz Zentrum Muenchen, Ingolstaedter Landstr. 1, 85764 Neuherberg, Germany.
Email: joel.schick@helmholtz-muenchen.de

Xiang Jin, Ministry of Education Key Laboratory for Ecology of Tropical Islands, Key Laboratory of Tropical Animal and Plant Ecology of Hainan Province, College of Life Sciences, Hainan Normal University, Haikou 571158, China.
Email: jinx@hainnu.edu.cn

Funding information
National Natural Science Foundation of China (NSFC), Grant/Award Number: 31860068; International Scientific and Technological Cooperation Project by Shihezi University, Grant/Award Number: GJHZ201708; Science and Technology Project of Bingtuan, Grant/Award Number: 2018AB012; Helmholtz Zentrum Muenchen GmbH (JAS)

Abstract

Species have evolved unique mechanisms to combat the effects of oxidative stress inside cells. A particularly devastating consequence of an unhindered oxidation of membrane lipids in the presence of iron results in cell death, known as ferroptosis. Hallmarks of ferroptosis, including peroxidation of polyunsaturated fatty acids, are conserved among animals and plants, however, early divergence of an ancestral mammalian GPX4 (mGPX4) has complicated our understanding of mechanistic similarities between species. To this end, we performed a comprehensive phylogenetic analysis and identified that orthologous *Arabidopsis* GPXs (AtGPXs) are more highly related to mGPX4 than mGPX4 is to other mammalian GPXs. This high degree of conservation suggested that experimental substitution may be possible. We, therefore, ectopically expressed AtGPX1-8 in ferroptosis-sensitive mouse fibroblasts. This substitution experiment revealed highest protection against ferroptosis induction by AtGPX5, as well as moderate protection by AtGPX2, −7, and −8. Further analysis of these cells revealed substantial abatement of lipid peroxidation in response to pharmacological challenge. The results suggest that the presence of ancestral GPX4 resulted in later functional divergence and specialization of GPXs in plants. The results also challenge a strict requirement for selenocysteine activity and suggest thioredoxin as a potent parallel antioxidant system in both plants and mammals.

KEYWORDS

reactive oxygen species, evolution, selenoprotein, thioredoxin, subcellular location

Abbreviations: aGPX, animal glutathione peroxidase; AtGPX, *Arabidopsis* glutathione peroxidase; aToc, α-tocopherol; GPX, glutathione peroxidase; GSH, glutathione; IKE, imidazole ketone erastin; mGPX, mammalian glutathione peroxidase; Mit, mitochondrion; PM, plasma membrane; ROS, reactive oxygen species; RSL3, ras-selective lethal small molecule 3 (1S, 3R); Sec, selenocysteine; Trx, thioredoxin.

Wangyang Song and Shan Xin contributed equally to this work.

1 | INTRODUCTION

Reactive oxygen species (ROS), such as singlet oxygen (O_2^1), superoxide (O_2^-), H_2O_2, and hydroxyl radicals, play significant roles in development, cell growth, and in response to environmental signaling.[1,2] High concentration of ROSs in living organisms lead to irreversible damage of different macromolecules such as proteins, lipids, and DNA.[3] Species have evolved enzymatic antioxidant system to combat the effects of oxidative stress inside cells, which includes superoxide dismutase (SOD), catalase (CAT), glutathione peroxidases (GPX), ascorbate peroxidase (APX), and glutathione reductase (GR).[4] In mammals, GPXs (EC 1.11.1.9) play a key role in protecting cells against oxidative damage, which are divided into five classes: cytosolic GPX (GPX1), gastrointestinal GPX (GPX2), plasma GPX (GPX3), phospholipid hydroperoxide GPX (GPX4), and seleno-independent epididymis GPXs (GPX5 and 6).[5] Mammalian GPX1−3, −5, and −6 act as homotetramers, while GPX4, −7, and −8 are functional as monomers.[6] Several mammalian GPXs (mGPXs) have selenium-dependent glutathione peroxidase activity, in which a selenocysteine (Sec) encoded by the opal TGA codon is present in the catalytic site.[7] Sec is considered as the 21st amino acid and the Sec site in mGPX4 has been shown to be required for preventing hydroperoxide-induced ferroptosis, an iron-dependent form of nonapoptotic cell death.[8]

In multicellular organisms, regulated cell death is one of the fundamental biological processes to eliminate damaged or unwanted cells.[9] Ferroptosis was first introduced to describe a nonapoptotic regulated cell death in 2012, which is characterized by iron-dependent, oxidative destruction of membrane polyunsaturated fatty acids.[10] The mechanism by which the small molecule erastin induces ferroptosis is believed to involve in glutathione (GSH) depletion through system Xc^- inhibition and consequently GPX4 inactivation.[11] GPX4 has been reported to play crucial roles in various diseases and development processes such as tumor growth, Parkinson's disease, and kidney degeneration through suppressing ferroptosis.[12-14] In addition to GSH and GPX4, several other metabolites and pathways are also believed to control ferroptosis sensitivity, including antioxidants coenzyme Q10 and tetrahydrobiopterin, NADPH and selenium abundance, and cysteine import.[15-18] Ferroptosis occurs when lipid peroxides (L-OOH) are fragmented into toxic lipid radicals (such as L-O·) and other reactive lipid breakdown products in the presence of ferric iron. GPX4 suppresses ferroptosis through reducing intracellular L-OOH to nontoxic lipid alcohols (L-OH), oxidizing the cofactor GSH in the process. It is believed that two factors are the most important for GPX4 to detoxify the lipid peroxides: (a) a selenocysteine in its active site and (b) its localization at the inner leaflet of the plasma membrane.[19] Targeted mutation of active Sec site of GPX4 (GPX4_U46S) resulted in embryonic lethality in female mice, indicating that the Sec is strictly required for GPX function in mammals.[20]

Plants have developed more complex antioxidation system compared to animals, due to their immobility and increased abiotic and/or biotic challenges. Plant GPXs play crucial roles in developmental, homeostatic, or stress-induced cell death.[21] The amino acid sequences of GPXs share high conservation in the GPX domains across various species, from microbe, plants to animals.[22] There are three conserved domains at the N-terminus: VNVAS(K/R/Q/E)CGLT, LAFPCNQF, and KWNF(E/T/A/S)KFLV, in which cysteine sites are localized at the active sites of GPXs.[23] Compared to mGPX4s, which use Sec as the active site, higher plants GPXs use Cys instead of Sec, leading to high affinity to thioredoxin (Trx) and very low affinity to GSH.[24] Thus, plants GPXs are actually Trx-dependent peroxidases, not GSH-dependent.[5] To date, all reported plant GPXs are functional as monomers, except in *Populus trichocarpa*, of which GPXs are homodimers.[25] As a well-studied peroxidase, characteristics of GPX families were reported in many plants, such as *Arabidopsis*, *Gossypium hirsutum*, *Thellungiella salsuginea*, *Lycopersicon esculentum* and *Helianthus annuus*, and *Rhodiola crenulata*.[5,26-29] Ferroptosis-like cell death was described in several plants, which were induced by heat shock (55°C, 10 minutes) and by interaction of rice and the pathogen *Magnaporthe oryzae*.[9,30] However, until now there has been no evidence linking GPXs to regulated ferroptosis-like cell death in plants, likely due to the differences between plant and animal cells, such as genetic redundancy, cell wall, different substrates usage (Trx and GSH), and different ferric ion functions.

Previous investigations have focused on GPX function either in animals or in plants. Yet, studies are lacking to connect the functional conservation of plant and animal GPXs to further link plant GPXs to ferroptosis. In this study, we performed a comprehensive evolutionary analysis of 254 GPXs obtained from bacteria to higher plants and vertebrates. The results revealed multiple origins of GPXs, as well as the patterns of expansion and loss of Sec-GPX in Chordata and higher plants. Functional analyses showed that AtGPX5 is particularly adept at protecting mammalian cells against ferroptosis, while −2, −7, and −8 can partially substitute. Differential pharmacological responses suggest AtGPX2 can protect mammalian cells from ferroptosis when using Trx as substrate, while AtGPX4 and −6, together with AtGPX2 and −5, can also protect cells from ferroptosis when using GSH. Here, we prove that GPXs are functionally conserved in ferroptosis protection in both animals and plants, providing a novel insight into the evolutionary origins of ferroptosis.

2 | MATERIALS AND METHODS

2.1 | Sequence acquisition

The genomes of different species were downloaded from NCBI Genome database (https://www.ncbi.nlm.nih.gov/genome/), JGI Phytozome database (https://phytozome.jgi.doe.gov/pz/portal.html), and Ensembl database (http://asia.ensembl.org/index.html). GPX protein sequences were obtained by a local BLAST program (blastp, e-value: 1×10^{-30}) using representative GPX sequences from model species. Output candidate GPXs were then analyzed to confirm the presence of the GSH peroxidase domain (IPR000889) using online tool InterProScan (http://www.ebi.ac.uk/interpro/search/sequence-search). Finally, a total of 254 GPXs were identified and used in the subsequent evolutionary analyses.

2.2 | Multiple sequence alignment and phylogenic analyses

The amino acid sequences of GPXs from different species were aligned using MUSCLE,[31] followed by phylogenetic tree construction using MEGA7.0[32] or TreeBeST (http://treesoft.sourceforge.net/treebest.shtml). Phylogenetic trees were constructed using the Neighbor-Joining method with 1000 bootstrapreplicates,andonlinetooliTOL(https://itol.embl.de/) was used for visualization.

The *Arabidopsis* GPX1−8 sequences were downloaded from TAIR database (https://www.arabidopsis.org) and subjected to ClustalW for multiple sequence alignment. The secondary structures of AtGPXs were predicted using RCSB PDB (http://www.rcsb.org/) and online tool ESPript3.0 (http://espript.ibcp.fr/ESPript/cgi-bin/ESPript.cgi) was used to generate the figures. The myristoylation sites were predicted by software Terminator (https://bioweb.i2bc.paris-saclay.fr/terminator3/).

2.3 | Vector construction

AtGPXs were purchased as murine codon-optimized gene fragments from TWIST Bioscience. Fragments were amplified by PCR to generate complementary overhangs for NEBuilder HiFi DNA Assembly Master Mix (E2621S, NEB). PCR fragments and pLVTHM (Addgene#12247), digested with PmeI/NdeI to replace EGFP with AtGPXs, were assembled according to the manufacturer's instructions. FLAG-tagged versions for localization were PCR amplified with universal forward primer from already existing constructs and re-assembled in pLVTHM backbone. All primers used in this work are listed in Table 1.

TABLE 1 Primers used in this work

Primers	Sequences (5′ to 3′)
AtGPX1 pLVTHM	acgagactagcctcgaggtttaaacgccaccatggtttccatgactacttcatc
AtGPX1 pLVTHM	ccagaggttgattatcatatgttaagcggcaagcaacttctgg
AtGPX2 pLVTHM	gagactagcctcgaggtttaaacgccaccatggcggatgaatctccaaagtc
AtGPX2 pLVTHM	atccagaggttgattatcatatgttaagaagaggcctgtcccaacgc
AtGPX3 pLVTHM	gagactagcctcgaggtttaaacgccaccatgcctagatcaagcagatgggt
AtGPX3 pLVTHM	atccagaggttgattatcatatgtcaagcagatgccaatagcttgac
AtGPX4 pLVTHM	cgagactagcctcgaggtttaaacgccaccatgggagcgagcgcatctgtgc
AtGPX4 pLVTHM	agaaggcactcgaggatgcctaacatatgataatcaacctctggattacaa
AtGPX5 pLVTHM	agactagcctcgaggtttaaacgccaccatgggtgcttcatcatcatcatct
AtGPX5 pLVTHM	tccagaggttgattatcatatgtcacaattcttgtgcaagggctt
AtGPX6 pLVTHM	gagactagcctcgaggtttaaacgccaccatgacgacaagtcaattcaagaagag
AtGPX6 pLVTHM	tccagaggttgattatcatatgctacaacaaccgaacagtctct
AtGPX7 pLVTHM	cgagactagcctcgaggtttaaacgccaccatggcattctcatacgccagtt
AtGPX7 pLVTHM	tcagaaacttctggcagcatgacatatgataatcaacctctggattacaa
AtGPX8 pLVTHM	cgagactagcctcgaggtttaaacgccaccatggccactaaagagccggaaag
AtGPX8 pLVTHM	gaacctgctcaacattagctagcatatgataatcaacctctggattacaa
mGpx4 pLVTHM	agactagcctcgaggtttaaacgccaccatgagctggggccgtctgagc
mGpx4 pLVTHM	tccagaggttgattatcatatgctagagatagcacggcaggtc
At1-6FLAG repair	cgagactagcctcgaggtttcttaccatggattacaaagacgatgacgataaaaacgccaccatg

2.4 | Ectopic expression of AtGPXs in mammalian cells

HeLa, mouse fibroblasts[33] were cultured in DMEM containing 10% FBS supplemented with 1% of L-Glutamine (Thermo Fisher Scientific, 25030024) and 1% of Penicillin-Streptomycin (Thermo Fisher Scientific, 15140122) at 37°C and 5% CO_2. Third generation ectopic lentiviruses were made using pHCMV-EcoEnv (Addgene plasmid #15802), pRSV-Rev (Addgene plasmid #12253), and pMDLg/pRRE (Addgene plasmid #12251) and the respective transfer vectors. HeLa cells were seeded the day before to reach 70% confluency and transfected with vector DNA mixed with XtremeGENE HP (Roche, 6366244001) transfection reagent in a ratio of 1:3 (DNA:reagent). Supernatant containing viral particles were collected after 72 hours, filtered through a 0.45 µmol/L syringe filter, and added to mouse fibroblast cells. After 48 hours of infection, cells were used in viability and lipid ROS assays. For confocal imaging, HeLa cells were transfected transiently with these constructs using Lipofectamine 2000 (Invitrogen) according to the manufacturer's instructions.

2.5 | Cell viability assays

Cells were seeded in 96-well plates and treated overnight with the respective compounds as indicated in figures and legends. A total of 2000 cells per well were added on top of wells containing ferroptosis inducers and incubated overnight. RSL3 and IKE were a kind gift from Brent Stockwell.

Viability was assessed by adding AquaBluer (MultiTarget Pharmaceuticals 6015) according to the manufacturer's instructions and fluorescence was measured at 540 nm excitation/emission 590 nm in an Envision 2104 Multilabel plate reader (PerkinElmer). Viability is reported as percentage relative to respective control treatment and averaged on at least three wells per condition.

2.6 | Analysis of lipid peroxides

Lipid reactive oxygen species (ROS) were detected using flow cytometry. First, 12 wells were seeded with 10,000 cells per well. The next day, medium was replaced with fresh medium containing either 0.5 µmol/L RSL3 or DMSO at the same dilution and incubated for 3 hours. Subsequently, cells were loaded with 2 µmol/L BODIPY 581/591 C11 (BODIPY-C11, Thermo Fisher Scientific D3861) in media for another 30 min at 37°C. Cells were washed with PBS before addition of Accutase (Sigma, A6964) to detach cells. Cells were resuspended in medium and 10,000 events collected per cell line on an Attune acoustic flow cytometer (Applied Biosystems) in BL-1 channel excited by the 488 nm laser. Histograms were created with FlowJo 10.

3 | RESULTS

3.1 | Phylogenetic analysis revealed multiple origins of animal GPXs

Protein sequences of reported GPXs from different representative species were obtained from GenBank and JGI database representing bacteria, archaea, fungi, lower plants, higher plants (Viridiplantae), and animals (from single cell to Metazoa). A total of 254 GPXs were finally selected and used in subsequent phylogenetic analysis (see Table S1 for detailed information). A holistic phylogenetic tree was built using NJ model and 1,000 bootstraps based on 233 representative GPXs (Figure 1). Self-organization of the phylogenetic tree resulted in a split into different clades according to species, except animal GPX4 (aGPX4) which formed a branch between fungus and lower plants, separating it from the other aGPX members (Figure 1). Two interesting findings could be deduced from this result. First, all plant GPXs are more closely related to aGPX4 than other animal GPXs, indicating that all plant GPXs and aGPX4 might have common origin. Second, aGPX4 and all plant GPXs are more closely related to species from early evolutionary history, such as fungi, bacteria, and archaea. Taken together, the phylogenetic analysis of representative GPXs showed that GPX4 may be the earliest GPX family member and comprises the origin of GPXs, while other GPXs only exist in animals by duplication and formed three sub-group of GPXs (aGPX1/2, aGPX7/8, and aGPX3/5/6, Figure 1).

The numbers of GPXs for a particular species to some extent reflect the functional diversity of GPXs. For all archaea, bacteria, and fungi investigated, only one GPX is identified for each species. In animals, all have more than four GPXs except two lower animals *Amphimedon queenslandica* (one GPX) and *Echinostoma caproni* (two GPXs). However, in lower plants investigated, only two algae species have more than three GPXs, *Chlamydomonas reinhardtii* and *Ectocarpus siliculosus* (Table S1 and Figure 1).

3.2 | Evolutionary analysis of GPXs showed Sec containing GPXs expanded in animals yet are absent from plants

As mentioned, the Sec sites of GPXs are crucial for the high enzyme activities of Sec-GPX in animals, while higher plants have no Sec-GPXs and show high affinity to Trx instead of GSH.[34,35] To illustrate the evolutionary patterns of this phenomenon, we constructed two phylogenetic trees for animals

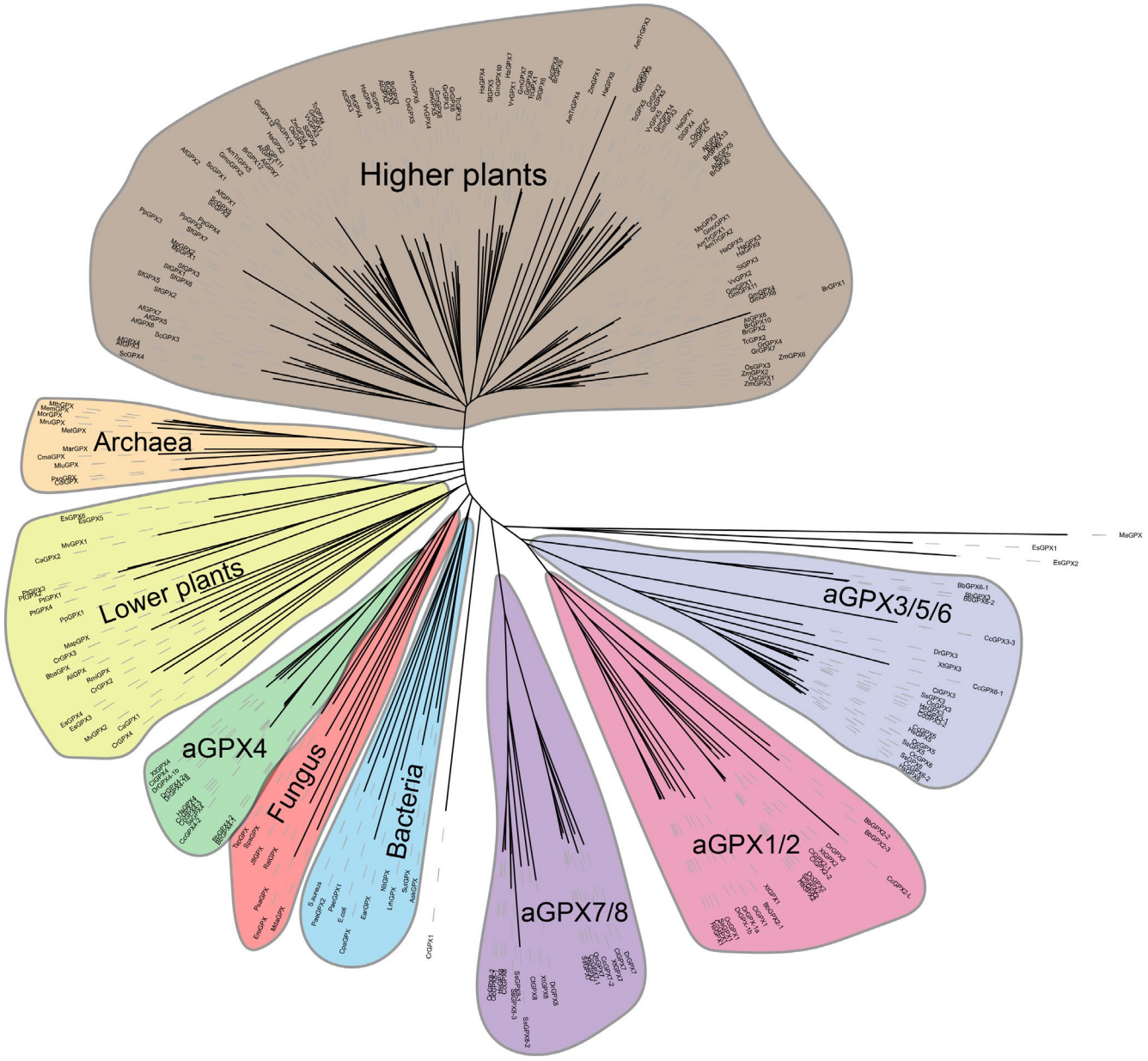

FIGURE 1 Phylogenetic tree of 233 representative GPX homologs from different species. Different color represented different taxa. The detailed information of those GPX sequences is listed in the Table S1. aGPX is the abbreviation of animal GPX. aGPX1/2 represents sub-group homolog to HsGPX1 and 2. Similar for aGPX7/8 and aGPX3/5/6

(80 aGPXs) and plants (79 GPXs), respectively. The results showed that in animals, the earliest Sec-GPX emerged in Cnidaria and particularly expanded in Chordata (Figure 2A). In contrast, Sec-GPX can only be observed in two algae species *E. siliculosus* and *C. reinhardtii*, the latter of which is considered the common ancestors of land plants (Figure 2B). Also, GPX gene family expansion events were observed in these two algae species, indicating that the Sec-GPXs may have emerged early through gene duplication events.

In the investigated plant other than algae, no Sec-GPX is found, indicating that these plants favored a GPX enzyme system with cysteine as active site and higher Trx affinity. Notably, in some higher plants (*Glycine max* and *Brassica rapa*), the numbers of GPXs for particular species are greater than ten, while no any Sec-GPX exists, indicating that the usage of Trx for plant GPXs must begin before the emergence of Viridiplantae common ancestor.

3.3 | Phylogenetic and subcellular localization analyses of AtGPXs indicated function diversity of different AtGPX members

To further investigate the sequence and functional diversity of GPXs from higher plants, a total of 100 GPXs from Viridiplantae were used to construct a phylogenetic tree.

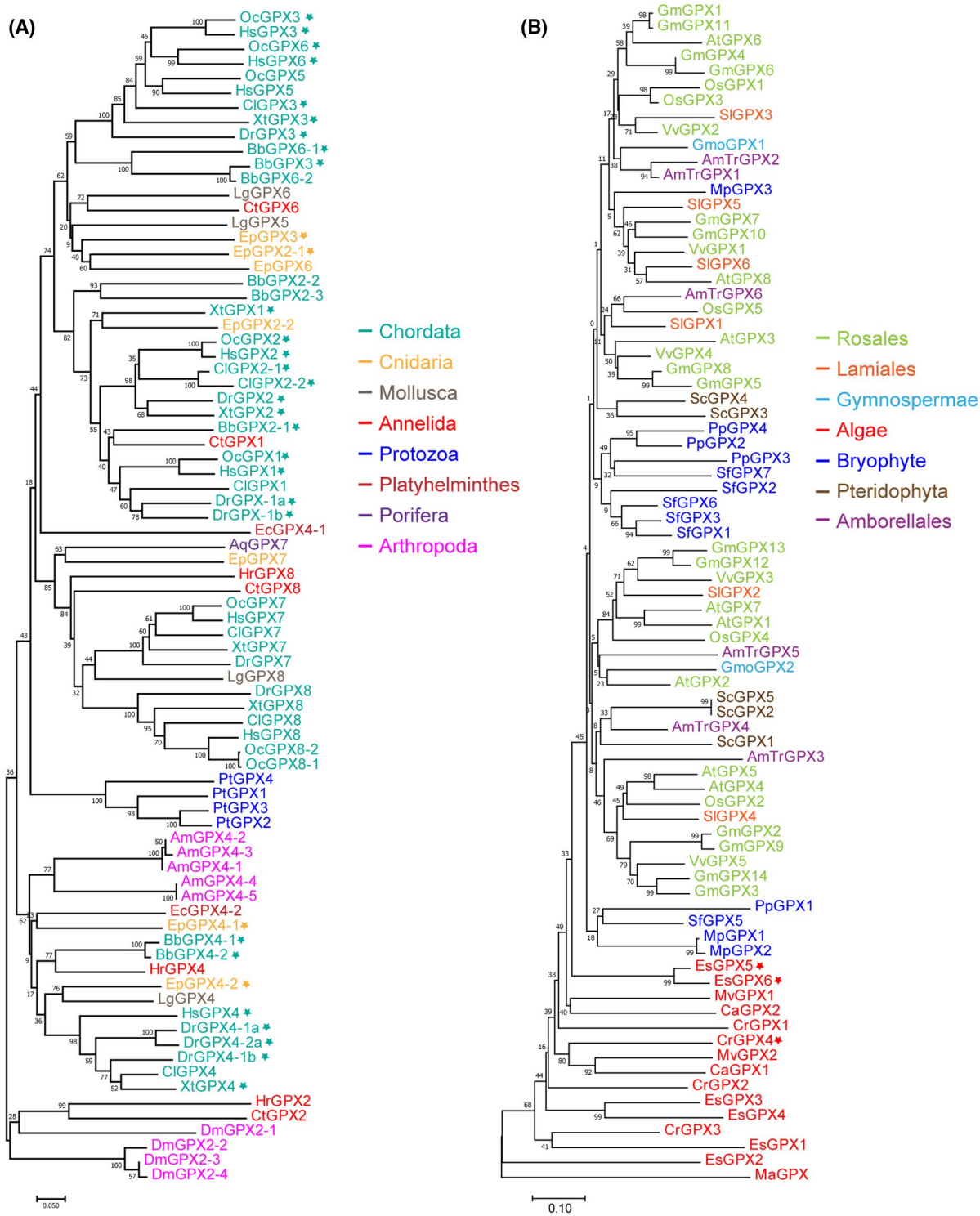

FIGURE 2 The evolution of GPXs in animals (A) and plants (B). Different colors represent different taxa. Asterisks indicate that corresponding proteins contain selenocysteine sites. The expansion and loss of Sec-GPX in animals and plants can be easily observed

Six well-supported sub-groups were observed in the phylogenetic tree of higher plants, corresponding to different sub-cellular localizations according to reported *Arabidopsis* GPX homologs (Figure 3A). Previously, it was shown that AtGPX3 was secretory/plasma membrane-bound while AtGPX4 and −5 were exclusively membrane-bound by myristoylation.[36] Both AtGPX5 and −6 have been considered localized to the plasma membrane, while AtGPX2

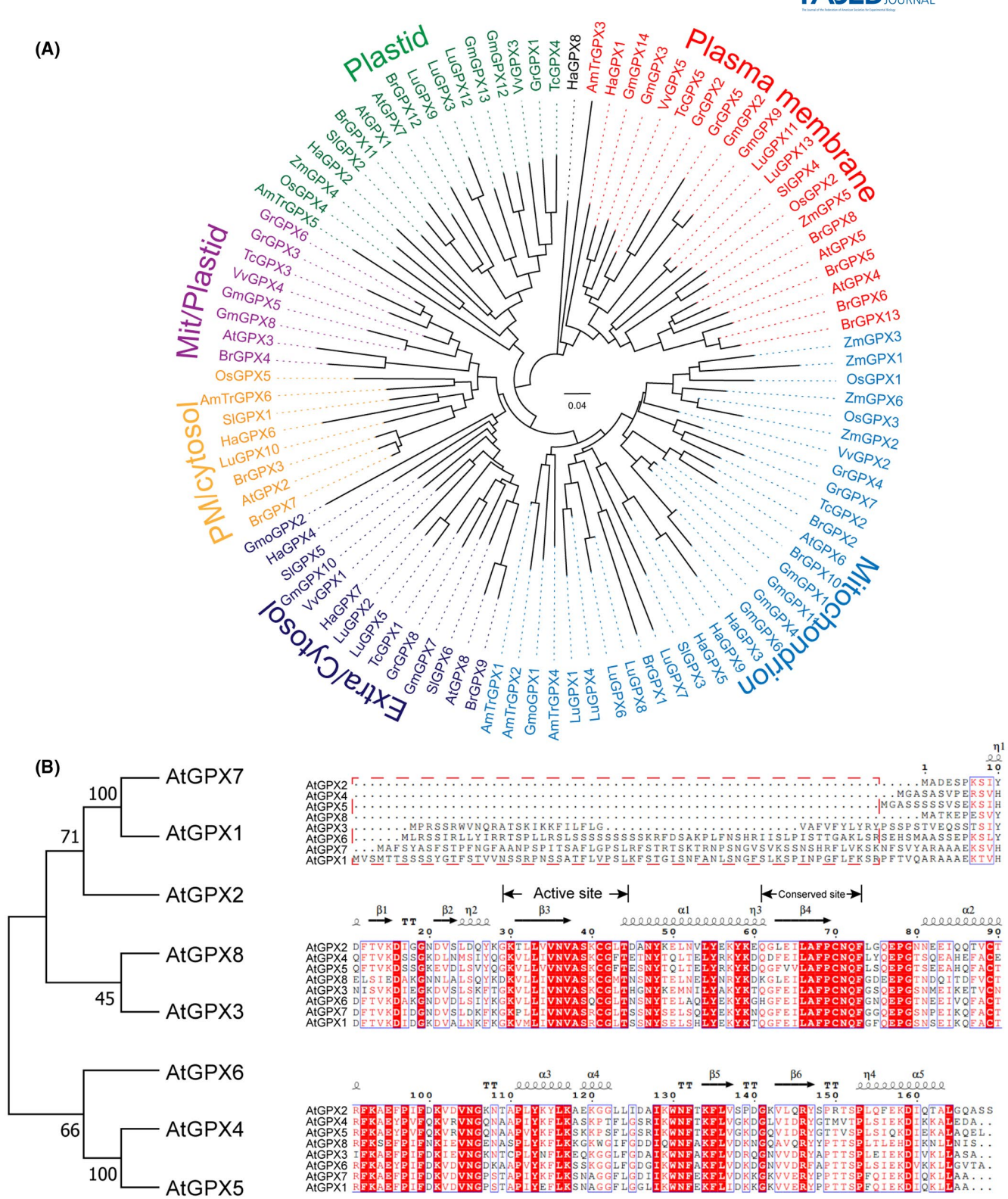

FIGURE 3 A, Phylogenetic tree of higher plant GPXs, (B) multiple sequence alignment of *Arabidopsis* GPXs, and (C) subcellular localization of AtGPXs expressed in mammalian cells. A, Different colors represent the different subcellular localization. Mit, mitochondrion; PM, plasma membrane. B, The protein secondary structure element symbols are presented on top (squiggles indicate α helices, arrows for β strands, and TT for β turns). Highly conserved amino acid residues are boxed and shadowed in red. The red dotted frame indicates potential signal peptides regions. The active site and conserved site also are shown on the top, respectively. Conserved domains are indicated by Roman numerals (I to III). Blue triangles indicate three crucial Cys residues for GPX activity. C, FLAG-tagged *Arabidopsis* GPX (AtGPX) protein localization in HeLa cells. A Cy3-labeled secondary antibody identifies each unique protein (red). Nuclei are labeled with DAPI (blue). White arrowheads indicate detectable membrane localization. Scale bar, 20 μm

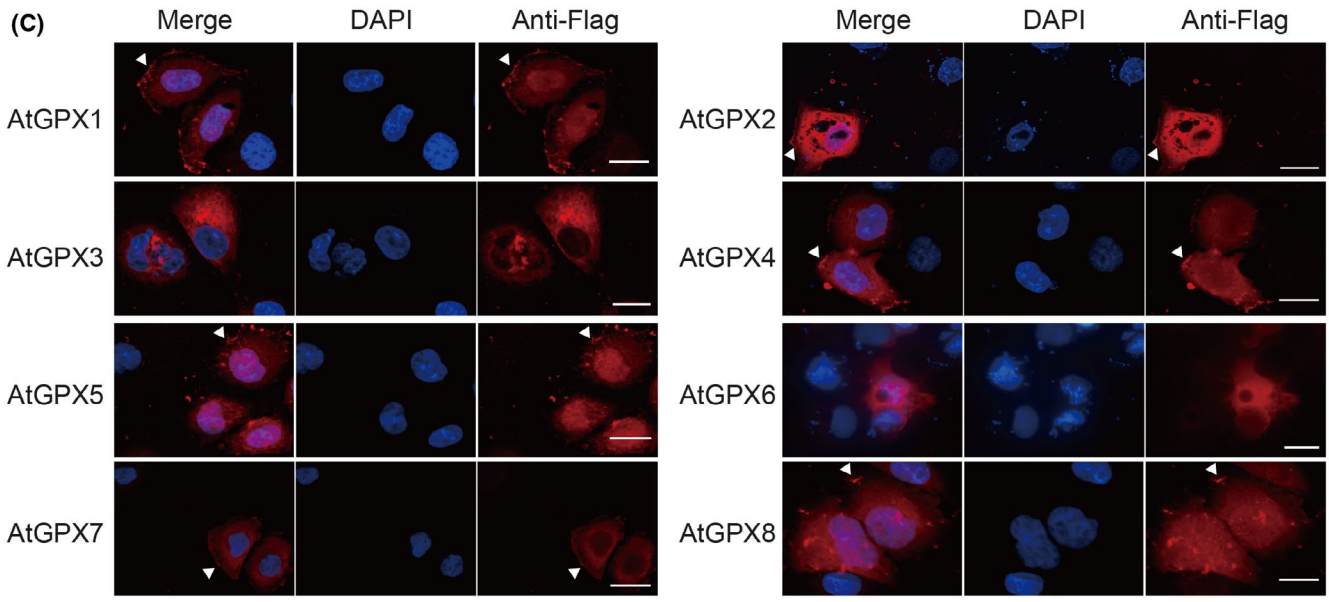

FIGURE 3 (Continued)

was found localized to both plasma membrane and cytosol,[37,38] indicating that AtGPXs might function in protecting the plasma membrane from oxidation, a key process in ferroptosis.

Multiple sequence alignment of eight AtGPXs showed high similarities in C-terminus but various N-terminuses (Figure 3B). Potential plastids-targeting peptides were found in AtGPX1 and −7. Mitochondria-targeting peptides and a N-terminal transmembrane domain were found in AtGPX6 and AtGPX3, respectively. The N-termini of both AtGPX4 and −5 contain the classical myristoylation motif MGxxxSxx, indicating possible membrane localization of these two paralogs (Figure 3B). No obvious signal peptides were observed in AtGPX2 and −8, consistent with their cytosolic localization. The conserved domains for AtGPXs are indicated, and three cysteine sites which are crucial for plant GPX activity are also indicated. Noted that the third cysteine site localizes in a predicted alpha-helix (not in a conserved domain), which is Gly, Trp, or Gln in aGPXs (Figure 3B).

Based on these results, we chose to test whether subcellular localization is conserved between kingdoms. We cloned AtGPX1−8 with an N-terminal FLAG tag into a lentiviral system for expression in mammalian cells and transfected these plasmids for transient expression into HeLa cells. Using antibodies directed against FLAG we detected predominately diffuse cytosolic localization for all proteins and additionally partial plasma membrane association for all AtGPX except AtGPX3 and −6 (Figure 3C). None of the proteins were exclusively localized to the plasma membrane, however, AtGPX3 showed a distinctive compartmentalization in the cytosol. This indicates that myristoylation sequences may only partially be used in mammalian cells, and that certain AtGPXs may depend on other proteins or scaffolding for membrane localization.

3.4 | Functional analysis revealed that AtGPX5 can potently protect against ferroptosis in mammalian cells

In light of the overlap in AtGPX subcellular localization and high sequence similarities between AtGPXs and mGPXs, we chose to examine whether any homologs could functionally protect against ferroptosis in mammalian cells. We used ferroptosis-sensitive mouse fibroblasts and two pharmacological inducers, (1S, 3R)-RSL3 (RSL3) a direct inhibitor of mGPX as well as imidazole ketone erastin (IKE), blocking system Xc^- (and decreasing cellular GSH levels). We generated separate cell pools expressing individual AtGPXs as well as mouse GPX4 as a positive control. Using the system, we challenged AtGPX lines in parallel and observed that AtGPX5 potently inhibited cell death induced by both RSL3 and IKE (Figure 4A,B). Weaker resistance was observed by homologs AtGPX2/7/8 against both substances, while AtGPX4 showed moderate protection against RSL3 and no protection against IKE. A similar result was observed for mGPX4, consistent with the mechanism of action of these two substances. RSL3 binds and indirectly inhibits mGPX4, while IKE blocks imports in production of the cofactor GSH. Thus, stoichiometric increases in mGPX4 can aid against the former but not the latter.

Ferroptosis execution is accompanied by widespread polyunsaturated fatty acid peroxidation. We chose to observe the effect of AtGPX expression on lipid peroxidation using

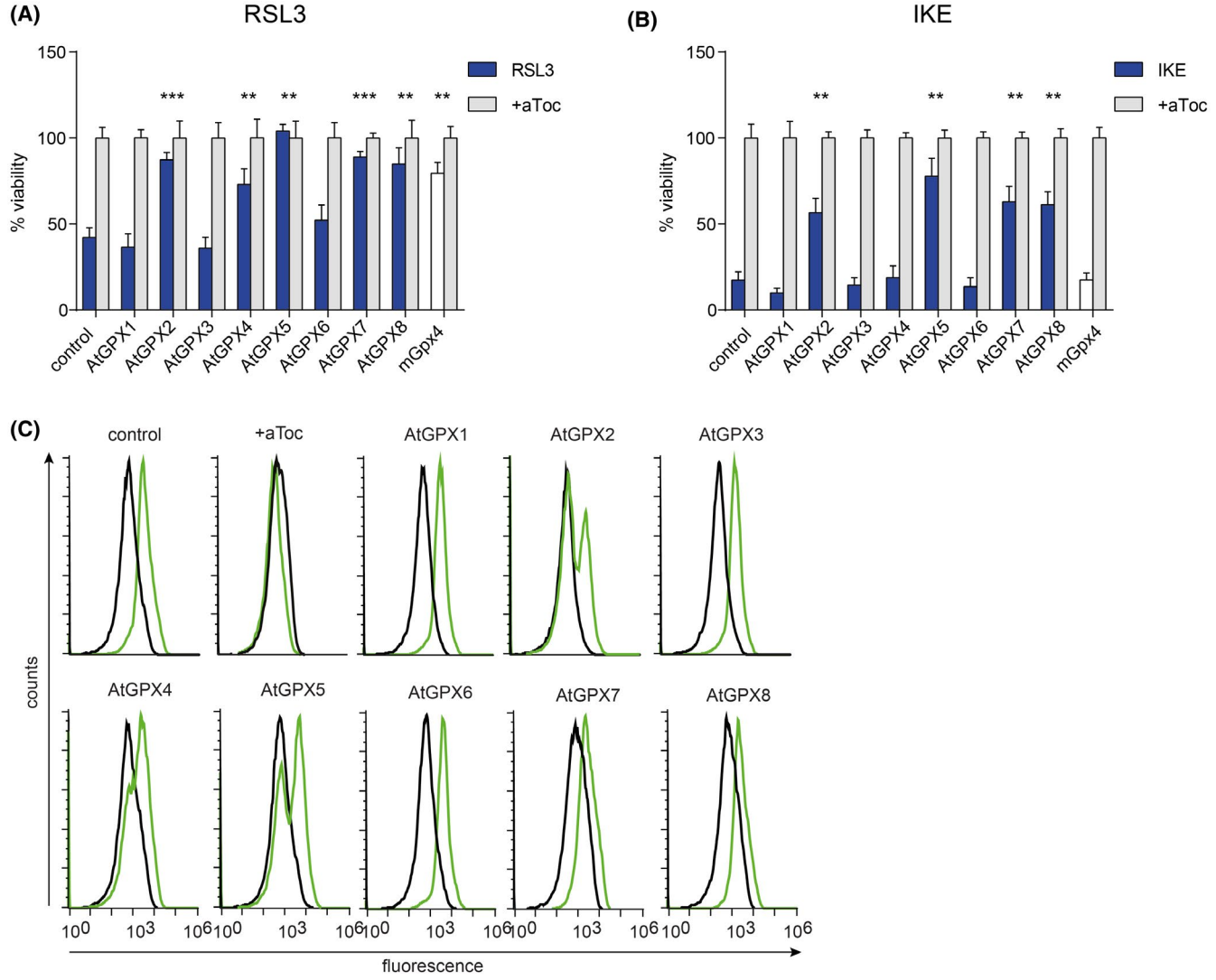

FIGURE 4 Resistance to ferroptosis in mammalian cells is mediated by specific *Arabidopsis* glutathione peroxidases. Overexpression of AtGPXs protects mouse embryonic fibroblasts against ferroptotic cell death induced by (A) RSL3 and (B) imidazole ketone erastin (IKE). Mouse Gpx4 (mGpx4) is included to demonstrate rescue by equivalent endogenous GPX4 activity. Mean values with SD of n = 4 technical replicates are shown. Statistics were calculated using one-way ANOVA. $^{**}P < .01$, $^{***}P < .001$. C, Lipid peroxidation induced by RSL3 in the same lines and measured by BODIPY 581/591 C11 (measured at 510 nm). The black line indicates untreated control cells. aToc, a-Tocopherol

BODIPY C11, a proxy for peroxidation at the membrane (Figure 4C). Following treatment of control cells with RSL3, a distinctive green fluorescence increase indicating peroxidation is observed, while antioxidant a-Tocopherol (aToc) completely protects membrane lipids against ferroptosis. Both AtGPX5 and AtGPX2 show emergence of peaks with limited oxidation as indicated by a shift toward unoxidized lipids in untreated (black) samples. In contrast, AtGPX7/8 did not produce a second peak but rather diminished the intensity of the oxidized peak. Interestingly, AtGPX4 slightly minimizes the lipid peroxidation. Together, these results indicate that AtGPX5 most potently protects against ferroptotic stimuli in mammalian cells, while AtGPX2/7/8 can partially protect. Strikingly, AtGPX4 similar to mGPX4 robustly protects only against RSL3, suggesting that it may use GSH as a cofactor.

4 | DISCUSSION

There are discrepancies as to the origin of GPXs. It has been reported that in mammals, the GPX family had evolved from a common ancestor of GPX4 by duplication events.[5] However, another evolutionary study claimed that vertebrate GPX1, −2, −3, −5, and −6 might have had a phylogenetic origin distinct from GPX4, indicating a multiple origin of aGPXs.[22] Our data support the latter theory that animal GPX1/2, GPX3/5/6, and GPX7/8 formed base branches in phylogenetic tree and have independent origins other than GPX4 (Figure 1). It also has been reported that mGPX4 is more closely related to fungi and lower plant GPXs than to other mammalian GPXs.[38] Our study showed similar results, demonstrating that the aGPX4 branch is close to bacteria,

fungi, and lower plants, and suggesting that GPX4 might be the earliest ancestral GPX member.

Selenium is one of the essential mineral elements for animals and human health.[39,40] Deficiency of selenium is associated with various human diseases, including but not limited to heart diseases, cystic fibrosis, Alzheimer's, and increased incidence of cancers.[41] Evidence is so far lacking regarding whether selenium is essential for vascular plants, however, it has been hypothesized that it may have beneficial biological functions in species that are able to accumulate high amounts of selenium.[42,43] Selenium is mainly distributed into selenium-containing proteins as Sec in mammals.[44] In prokaryotes, selenium also occurs as Sec, as well as a catalytically essential cofactor in other selenoproteins.[45,46] However, plants appear to divert selenium rather than accumulate Sec and selenomethionine, which leads to high tolerance of selenium content.[47] This may partly explain that why plants discarded Sec-GPX during evolutionary history (Figure 2B), in that plants need to avoid potential selenium toxicity occurring in natural soil with greater selenium availability. Selenium levels and atmospheric oxygen are associated with major extinction events, also providing a potential evolutionary context to Sec-GPX depletion.[48] Animals, in contrast, are migratory and choose their diets, providing a possible explanation for the expansion of Sec-GPX in Chordata (Figure 2A). In addition, when Trx acts as the electronic donor for GPXs instead of GSH, Cys-GPXs have high activity.[49] The fact that Trx is widespread in non-vertebrate organisms, green plants, bacteria, and fungi supported the evolutionary analysis results in this work that Sec-GPXs were observed mainly in Chordata and algae (Figures 1 and 2).[50,51] In this context, it is surprising that AtGPX5 and AtGPX2/7/8 can protect although they are mostly localized to the cytosol. This may suggest that efficiently detoxifying peroxides in the cytosol may contribute secondarily to fewer lipid peroxides. We believe that the living strategies that different species choose to adapt to the environment of earth during evolutionary history lead to the different Sec-GPX distribution patterns in various organisms. The theory that plants GPXs use Trx as electron donor might partly explain ferroptosis rescue of AtGPX5 and AtGPX2/7/8 in mammalian cells when IKE was applied, which can deplete cellular GSH. Consistent with this observation, it was recently reported that ferroptocide, an inhibitor of Trx, can rapidly and robustly induce ferroptotic death in cancer cells, underlining the concept that Trx also plays important roles in ferroptosis pathway in mammalian cells.[52]

Functional diversity of similar paralogue proteins usually links to their subcellular localization with different microenvironment.[53] Previous work described the subcellular localization of all GPXs in *A. thaliana* using both in silico and in vivo approaches.[37] Consistent with the bioinformatics analysis, the subcellular localization in *Arabidopsis* of AtGPX1 and −7 are to the plastids; AtGPX2 and −8 are localized to the cytosol; the N-terminal peptide of AtGPX6 targets it to mitochondria; AtGPX3 is found exclusively in the secretory pathway, anchored by a single transmembrane domain; and AtGPX4 and −5 are anchored to the plasma membrane.[36] Similarly, plastid target signals, membrane localization signals (N-terminal myristoylation sites), and mitochondria target signals were identified from corresponding AtGPX members in this work (Figure 3B). As we observed, the amino acid sequences of plant and animal GPXs are highly conserved, although they are thought to use different substrates as electron donors. The catalytic mechanisms of animal and plant GPXs depend on the Sec and Cys active site they use, however, the functional conservation, especially the functions regarding ferroptosis, of plant and animal GPXs were not clearly investigated.

Here, we provided the first functional and subcellular investigation of AtGPXs in mammalian cells, demonstrating that related AtGPX members could protect mammalian cells from ferroptosis with different efficiencies. In all cases, both animal and plant homologs require membrane localization in order to reduce oxidized lipids responsible for executing ferroptosis. Consistently, we observed that in addition to widespread cytosolic staining, AtGPX1, −2, −4, −5 −7, and −8 are at least partially localized to the plasma membrane. Notably, plastid localized AtGPX1 and −7 showed universal distribution in mammalian cells due to the lack of plastids (Figure 3C). One interesting finding is that highly similar paralogues AtGPX4 and −5 showed different protection efficiency following IKE treatment (Figure 4A). It is possible that this difference is due to efficiency of myristoylation in mammalian cells. Similar results were observed between AtGPX2, −7, and −8, due to unknown mechanisms (Figure 4A,B), which may possibly include sequestration to the membrane by cofactors, and warrant further investigation into this mechanism. These findings will help to better understand animal and plant GPXs' functions in regulated cell death. Up to date, few original research articles have reported ferroptotic cell death in plants, largely because plants have much higher capacity to clear ROS toxic than animals. However, ferroptotic cell death definitely executes an important role in plants, at least in heat stress response[9] and in response to diseases.[30,54] Certainly the functions of ferroptotic cell death in plants in the future will become a subject of intense investigation.

Strikingly, AtGPX5 expression protects cells even better than the endogenous mGPX4. Whether this due to localization or better reducing capacity or availability of the Trx system remains to be investigated. However, lipid peroxides as evinced by BODIPY staining are more potently reduced by AtGPX2. This may additionally suggest that AtGPX5 may have more specific lipid substrates for detoxification. However, more investigation should be performed in the

future on plant GPXs' functions in ferroptosis, which will help a lot to better understand the evolution meaning of this kind of regulated cell death.

In conclusion, GPXs play key roles in anti-oxidative damage in many species. In this study, we provided a comprehensive evolutionary analysis of 254 GPXs of various species from bacteria to higher plants and vertebrates. The results supported the theory that aGPXs have different origins and all plant GPXs are evolved from a common ancestor similar to aGPX4. Further sequence analysis revealed that animal Sec-GPX first emerged in Cnidaria and particularly expanded in Chordata, while in plants Sec-GPX can only be observed in algae species and is lost in higher plants. Sequence and functional analyses revealed that highest protection against ferroptosis was inducted by AtGPX5, as well as moderate protection by AtGPX2, −7, and −8. Further analysis of the transformed cells revealed substantial abatement of lipid peroxidation in response to pharmacological challenge. These findings lead to the conclusion that GPXs are functionally conserved in ferroptosis protection in both animals and plants, which will provide better understanding of the evolutionary meaning of ferroptosis.

ACKNOWLEDGMENTS

This work was supported by the National Natural Science Foundation of China, grant number 31860068, International Scientific and Technological Cooperation project by Shihezi University, grant number GJHZ201708, Science and Technology Project of Bingtuan, grant number 2018AB012, and Helmholtz Zentrum Muenchen GmbH (JAS). The authors also want to thank for the support from the academician workstation of Hainan Province.

AUTHOR CONTRIBUTIONS

H. Li, J.A. Schick, and X. Jin designed the research; W. Song, S. Xin, and M. He performed the main experiment and data analysis; S. Pfeiffer conducted experiments, analyzed data, and provided key reagents; H. Li, J.A. Schick, and X. Jin supervised the study and obtained funding; A. Cao and H. Li wrote the original draft; J.A. Schick and X. Jin review and editing the final manuscript; all authors read and approved the final version of the manuscript.

ORCID

Joel A. Schick https://orcid.org/0000-0002-8623-4910

REFERENCES

1. Finkel T. Oxygen radicals and signaling. *Curr Opin Cell Biol*. 1998;10:248-253.
2. Mittler R, Vanderauwera S, Gollery M, Van Breusegem F. Reactive oxygen gene network of plants. *Trends Plant Sci*. 2004;9:490-498.
3. Imlay JA, Linn S. DNA damage and oxygen radical toxicity. *Science*. 1988;240:1302-1309.
4. Roxas VP, Lodhi SA, Garrett DK, Mahan JR, Allen RD. Stress tolerance in transgenic tobacco seedlings that overexpress glutathione S-transferase/glutathione peroxidase. *Plant Cell Physiol*. 2000;41:1229-1234.
5. Herbette S, Roeckel-Drevet P, Drevet JR. Seleno-independent glutathione peroxidases. More than simple antioxidant scavengers. *FEBS J*. 2007;274:2163-2180.
6. Ursini F, Maiorino M, Gregolin C. The selenoenzyme phospholipid hydroperoxide glutathione peroxidase. *Biochim Biophys Acta*. 1985;839:62-70.
7. Rotruck JT, Pope AL, Ganther HE, Swanson AB, Hafeman DG, Hoekstra WG. Selenium: biochemical role as a component of glutathione peroxidase. *Science*. 1973;179:588-590.
8. Ingold I, Berndt C, Schmitt S, et al. Selenium utilization by GPX4 is required to prevent hydroperoxide-induced ferroptosis. *Cell*. 2018;172:409-422.e21.
9. Distefano AM, Martin MV, Cordoba JP, et al. Heat stress induces ferroptosis-like cell death in plants. *J Cell Biol*. 2017;216:463-476.
10. Dixon SJ, Lemberg KM, Lamprecht MR, et al. Ferroptosis: an iron-dependent form of nonapoptotic cell death. *Cell*. 2012;149:1060-1072.
11. Yang WS, SriRamaratnam R, Welsch ME, et al. Regulation of ferroptotic cancer cell death by GPX4. *Cell*. 2014;156:317-331.
12. Van Do B, Gouel F, Jonneaux A, et al. Ferroptosis, a newly characterized form of cell death in Parkinson's disease that is regulated by PKC. *Neurobiol Dis*. 2016;94:169-178.
13. Jiang L, Kon N, Li T, et al. Ferroptosis as a p53-mediated activity during tumour suppression. *Nature*. 2015;520:57-62.
14. Friedmann Angeli JP, Schneider M, Proneth B, et al. Inactivation of the ferroptosis regulator Gpx4 triggers acute renal failure in mice. *Nat Cell Biol*. 2014;16:1180-1191.
15. Angeli JPF, Shah R, Pratt DA, Conrad M. Ferroptosis inhibition: mechanisms and opportunities. *Trends Pharmacol Sci*. 2017;38:489-498.
16. Cardoso BR, Hare DJ, Bush AI, Roberts BR. Glutathione peroxidase 4: a new player in neurodegeneration? *Mol Psychiatry*. 2017;22:328-335.
17. Shimada K, Skouta R, Kaplan A, et al. Global survey of cell death mechanisms reveals metabolic regulation of ferroptosis. *Nat Chem Biol*. 2016;12:497-503.
18. Kraft VAN, Bezjian CT, Pfeiffer S, et al. GTP cyclohydrolase 1/tetrahydrobiopterin counteract ferroptosis through lipid remodeling. *ACS Cent Sci*. 2020;6:41-53.
19. Imai H, Nakagawa Y. Biological significance of phospholipid hydroperoxide glutathione peroxidase (PHGPx, GPx4) in mammalian cells. *Free Radic Biol Med*. 2003;34:145-169.
20. Ingold I, Aichler M, Yefremova E, et al. Expression of a catalytically inactive mutant form of glutathione peroxidase 4 (Gpx4) confers a dominant-negative effect in male fertility. *J Biol Chem*. 2015;290:14668-14678.
21. Conlon M, Dixon SJ. Ferroptosis-like death in plant cells. *Mol Cell Oncol*. 2017;4:e1302906.
22. Margis R, Dunand C, Teixeira FK, Margis-Pinheiro M. Glutathione peroxidase family – an evolutionary overview. *FEBS J*. 2008;275:3959-3970.
23. Iqbal A, Yabuta Y, Takeda T, Nakano Y, Shigeoka S. Hydroperoxide reduction by thioredoxin-specific glutathione peroxidase isoenzymes of *Arabidopsis* thaliana. *FEBS J*. 2006;273:5589-5597.

24. Lubos E, Loscalzo J, Handy DE. Glutathione peroxidase-1 in health and disease: from molecular mechanisms to therapeutic opportunities. *Antioxid Redox Signal*. 2011;15:1957-1997.
25. Koh CS, Didierjean C, Navrot N, et al. Crystal structures of a poplar thioredoxin peroxidase that exhibits the structure of glutathione peroxidases: insights into redox-driven conformational changes. *J Mol Biol*. 2007;370:512-529.
26. Chen M, Li K, Li H, Song CP, Miao Y. The glutathione peroxidase gene family in gossypium hirsutum: genome-wide identification, classification, gene expression and functional analysis. *Sci Rep*. 2017;7:44743.
27. Gao F, Chen J, Ma T, et al. The glutathione peroxidase gene family in Thellungiella salsuginea: genome-wide identification, classification, and gene and protein expression analysis under stress conditions. *Int J Mol Sci*. 2014;15:3319-3335.
28. Passaia G, Queval G, Bai J, Margis-Pinheiro M, Foyer CH. The effects of redox controls mediated by glutathione peroxidases on root architecture in *Arabidopsis* thaliana. *J Exp Bot*. 2014;65:1403-1413.
29. Zhang L, Wu M, Yu D, et al. Identification of glutathione peroxidase (GPX) gene family in rhodiola crenulata and gene expression analysis under stress conditions. *Int J Mol Sci*. 2018;19:3329.
30. Dangol S, Chen Y, Hwang BK, Jwa NS. iron- and reactive oxygen species-dependent ferroptotic cell death in rice-magnaporthe oryzae interactions. *Plant Cell*. 2019;31:189-209.
31. Edgar RC. MUSCLE: a multiple sequence alignment method with reduced time and space complexity. *BMC Bioinformatics*. 2004;5:113.
32. Kumar S, Stecher G, Tamura K. MEGA7: molecular evolutionary genetics analysis version 7.0 for bigger datasets. *Mol Biol Evol*. 2016;33:1870-1874.
33. Seiler A, Schneider M, Forster H, et al. Glutathione peroxidase 4 senses and translates oxidative stress into 12/15-lipoxygenase dependent- and AIF-mediated cell death. *Cell Metab*. 2008;8:237-248.
34. Hazebrouck S, Camoin L, Faltin Z, Strosberg AD, Eshdat Y. Substituting selenocysteine for catalytic cysteine 41 enhances enzymatic activity of plant phospholipid hydroperoxide glutathione peroxidase expressed in *Escherichia coli*. *J Biol Chem*. 2000;275:28715-28721.
35. Maiorino M, Aumann KD, Brigelius-Flohe R, et al. Probing the presumed catalytic triad of selenium-containing peroxidases by mutational analysis of phospholipid hydroperoxide glutathione peroxidase (PHGPx). *Bio Chem Hoppe-Seyler*. 1995;376:651-660.
36. Attacha S, Solbach D, Bela K, et al. Glutathione peroxidase-like enzymes cover five distinct cell compartments and membrane surfaces in *Arabidopsis* thaliana. *Plant Cell Environ*. 2017;40:1281-1295.
37. Bela K, Horvath E, Galle A, Szabados L, Tari I, Csiszar J. Plant glutathione peroxidases: emerging role of the antioxidant enzymes in plant development and stress responses. *J Plant Physiol*. 2015;176:192-201.
38. Passaia G, Margis-Pinheiro M. Glutathione peroxidases as redox sensor proteins in plant cells. *Plant Sci*. 2015;234:22-26.
39. Rayman MP. Selenium and human health. *Lancet*. 2012;379:1256-1268.
40. White PJ, Brown PH. Plant nutrition for sustainable development and global health. *Ann Bot*. 2010;105:1073-1080.
41. Fairweather-Tait SJ, Bao Y, Broadley MR, et al. Selenium in human health and disease. *Antioxid Redox Signal*. 2011;14:1337-1383.
42. Djanaguiraman M, Devi DD, Shanker AK, Sheeba JA, Bangarusamy U. Selenium–an antioxidative protectant in soybean during senescence. *Plant Soil*. 2005;272:77-86.
43. Terry N, Zayed AM, De Souza MP, Tarun AS. Selenium in higher plANTS. *Annu Rev Plant Physiol Plant Mol Biol*. 2000;51:401-432.
44. Burk RF, Hill KE. Regulation of Selenium Metabolism and Transport. *Annu Rev Nutr*. 2015;35:109-134.
45. Gladyshev VN, Khangulov SV, Stadtman TC. Nicotinic acid hydroxylase from Clostridium barkeri: electron paramagnetic resonance studies show that selenium is coordinated with molybdenum in the catalytically active selenium-dependent enzyme. *Proc Natl Acad Sci USA*. 1994;91:232-236.
46. Kieliszek M, Blazejak S, Gientka I, Bzducha-Wrobel A. Accumulation and metabolism of selenium by yeast cells. *Appl Microbiol Biotechnol*. 2015;99:5373-5382.
47. White PJ. Selenium accumulation by plants. *Ann Bot*. 2016;117:217-235.
48. Long JA, Large RR, Lee MSY, et al. Severe selenium depletion in the Phanerozoic oceans as a factor in three global mass extinction events. *Gondwana Res*. 2016;36:209-218.
49. Navrot N, Collin V, Gualberto J, et al. Plant glutathione peroxidases are functional peroxiredoxins distributed in several subcellular compartments and regulated during biotic and abiotic stresses. *Plant Physiol*. 2006;142:1364-1379.
50. Herbette S, Lenne C, Leblanc N, Julien JL, Drevet JR, Roeckel-Drevet P. Two GPX-like proteins from Lycopersicon esculentum and Helianthus annuus are antioxidant enzymes with phospholipid hydroperoxide glutathione peroxidase and thioredoxin peroxidase activities. *Eur J Biochem*. 2002;269:2414-2420.
51. Maiorino M, Ursini F, Bosello V, et al. The thioredoxin specificity of Drosophila GPx: a paradigm for a peroxiredoxin-like mechanism of many glutathione peroxidases. *J Mol Biol*. 2007;365:1033-1046.
52. Llabani E, Hicklin RW, Lee HY, et al. Diverse compounds from pleuromutilin lead to a thioredoxin inhibitor and inducer of ferroptosis. *Nat Chem*. 2019;11:521-532.
53. Gardy JL, Brinkman FS. Methods for predicting bacterial protein subcellular localization. *Nat Rev Microbiol*. 2006;4:741-751.
54. Shen Q, Liang M, Yang F, Deng YZ, Naqvi NI. Ferroptosis contributes to developmental cell death in rice blast. *New Phytol*. 2020;227:1831-1846.

SUPPORTING INFORMATION

Additional Supporting Information may be found online in the Supporting Information section.

How to cite this article: Song W, Xin S, He M, et al. Evolutionary and functional analyses demonstrate conserved ferroptosis protection by *Arabidopsis* GPXs in mammalian cells. *The FASEB Journal*. 2021;35:e21550. https://doi.org/10.1096/fj.202000856R